Contribution from the Department of Chemistry,
Brookhaven National Laboratory, Upton, New York 11973

Homogeneous Catalysis of the Water Gas Shift Reaction by (Polypyridine)rhodium Complexes

DEVINDER MAHAJAN, CAROL CREUTZ,* and NORMAN SUTIN

Received September 14, 1984

Homogeneous catalysis of the water gas shift reaction under mild conditions (<100 °C (1 atm CO)) has been achieved with several (polypyridine)rhodium(I) complexes as catalyst precursors (polypyridine = 2,2′-bipyridine (bpy), 1,10-phenanthroline, pyrazine, 4,4′-dimethyl-2,2′-bipyridine), in alcohol–water mixtures. The complex $Rh(bpy)_2^+$ was found to be the most active catalyst precursor (~3 turnovers/h at 90° C). In buffered water–ethanol (22:3) mixtures, the rates of H_2 and CO_2 production were highest at pH ~3. The pH dependence of the rates and solution UV spectra in the latter medium implicate $Rh(bpy)_2(CO)H^{2+}$ as the catalyst; this species predominates below pH 3 and exhibits hydroxide-promoted activity suggestive of a metallocarboxylic acid mechanism. At pH >3, the rhodium(I) species present exhibit little catalytic activity.

Introduction

The water gas shift (WGS) reaction, eq 1, which is presently used on an industrial scale to augment the hydrogen content of water gas (synthesis gas) produced from the combustion of coal,

$$H_2O + CO \overset{K}{\rightleftharpoons} H_2 + CO_2 \qquad (1)$$

is catalyzed heterogeneously by metal oxides at elevated temperatures.[1] From the thermodynamics[2] (K = 1450 and 26.9 at 400 and 600 K, respectively; ΔH°_{298} = 0.68 kcal mol^{-1}; ΔG°_{298} = −4.76 kcal mol^{-1}; ΔS°_{298} = +18.3 cal deg^{-1} mol^{-1} for $H_2O(l)$ in eq 1) it is clear that low temperature is desirable for the efficiency of this reaction. Since homogeneous catalysis affords this possibility, homogeneous catalysts for the reaction are currently being sought. Transition-metal complexes that have been examined include the carbonyls $Ru_3(CO)_{12}$,[3] $M(CO)_6$ (M = Cr, Mo, W),[4] $Fe(CO)_5$,[4a,5] and $Rh_6(CO)_{16}$,[3b,c] phosphine and amine complexes $RhHL_3$,[6] $[Ir(diene)L_2]^+$ (L = monodentate or L_2 = bidentate ligands with phosphorus or nitrogen donor atoms),[7] the $[Rh(CO)_2Cl]_2$–NaI system,[8] and mixed-metal systems, e.g. $K_2PtCl_4/SnCl_4 \cdot 5H_2O$.[9] A light-assisted catalysis of the WGS reaction has also been reported with the $[Ru(Cl)(CO)(bpy)_2]Cl$ complex.[10]

While studying the activation of small molecules (e.g., CO, H_2, etc.) by $Rh(bpy)_2^+$ (2,2′-bipyridine = bpy),[11,12] we found that the rhodium(I) complex is a catalyst precursor for the WGS reaction under mild conditions (<100 °C (<1 atm CO)). Here, we report results from our study of $Rh(bpy)_2^+$ and some related complexes as WGS catalysts. While this work was in progress, a report on a closely related system was published.[13] Our observations are generally in accord with those in ref 13 and provide information bearing on the mechanism of the WGS reaction in the rhodium–bipyridine system.

Experimental Section

Materials. AR grade solvents were distilled according to literature methods and were vacuum degassed before use. Rhodium trichloride trihydrate was purchased from Alfa. 2,2′-Bipyridine (bpy), 1,10-phenanthroline (phen), and 4,4′-dimethyl-2,2′-bipyridine (Me_2bpy) from G. F. Smith and pyrazine from Aldrich were used as received. CO, H_2, CO_2, and Ar gases were from either Matheson or Union Carbide. In a few experiments CO was passed through a Cr(II) scrubbing tower to remove traces of O_2. H_2 gas was purified by passing through Engelhard's "Deoxo Catalytic Purifier". Triply distilled or Milli-Q water was used in all experiments.

The rhodium complexes $[Rh(CO)_2Cl]_2$,[14] $[Rh(bpy)_2]Cl$,[12] $[Rh(phen)_2]Cl$,[12] $[Rh(bpy)_2]ClO_4$,[15] $[Rh(CO)_2Cl]_2(\mu\text{-pz})$,[16] $[Rh(CO)_2Cl]_2(\mu\text{-bpy})$,[17] $[Rh(bpy)_3](ClO_4)_3$,[11] $[Rh(bpy)_2(H_2O)_2](ClO_4)_3$,[11] $[Rh(bpy)(CO)_2]ClO_4$,[18] and $Rh(bpy)(CO)(H)(Cl)_2$[19] were prepared by literature methods. The sulfate salt of $Rh(bpy)_2^+$ was prepared by passing a saturated solution of $[Rh(bpy)_2]Cl$ in 2:1 ethanol–water through an anion-exchange column (Dowex sulfate form, 1 × 8, 100–200 mesh) followed by evaporation of the effluent on a rotary evaporator.

The reaction of $[Rh(CO)_2Cl]_2$ with bpy (bpy:Rh > 1) in benzene immediately gave a blue solid, but on further stirring, the blue solid disappeared and a dark brown solid separated. The brown solid was filtered, washed with benzene a few times, and dried in vacuo. IR (Nujol mull): ν(CO) 2080, 2060, 2020, 1980, 1830, 1810 cm^{-1}.

Methods. All reactions and manipulations were carried out under an atmosphere of Ar, using glovebox[12] or Schlenk techniques. The WGS reaction was carried out in a glass flask with two side arms at an angle to each other. One arm, topped by a large-bore glass stopcock capped with a septum, allowed for gas-phase sampling while the second arm could be attached to a vacuum line for adding gas to, or pumping it from, the solution. In a typical glovebox experiment the rhodium complex was

(1) See e.g.: Thomas, C. L. "Catalytic Processes and Proven Catalysts"; Academic Press: New York, 1970.
(2) These values were taken from: Ford, P. C. *Acc. Chem. Res.* **1981**, *14*, 31.
(3) (a) Laine, R. M.; Rinker, R. G.; Ford, P. C. *J. Am. Chem. Soc.* **1977**, *99*, 252. (b) Ungermann, C.; Landis, V.; Moya, S. A.; Cohen, H.; Walker, H.; Pearson, R. G.; Rinker, R. G.; Ford, P. C. *J. Am. Chem. Soc.* **1979**, *101*, 5922. (c) Ford, P. C.; Rinker, R. G.; Laine, R. M.; Ungerman, C.; Landis, V.; Moya, S. A. *Adv. Chem. Ser.* **1979**, *No.* **173**, 81. (d) Gross, D. C.; Ford, P. C. Second North American Chemical Congress, Las Vegas, NV, Aug 1980.
(4) (a) King, R. B.; Frazier, C. C.; Hanes, R. M.; King, A. D., Jr. *J. Am. Chem. Soc.* **1978**, *100*, 2925. (b) King, A. D., Jr.; King, R. B.; Sailers, E. L., III *J. Am. Chem. Soc.* **1981**, *103*, 1867. (c) King, A. D., Jr.; King, R. B.; Yang, D. B. *J. Am. Chem. Soc.* **1981**, *103*, 2699 and references cited therein. (d) Pearson, R. G.; Mauermann, H. *J. Am. Chem. Soc.* **1982**, *104*, 500.
(5) (a) King, A. D., Jr.; King, R. B.; Yang, D. B. *J. Am. Chem. Soc.* **1980**, *102*, 1028 and references therein. (b) Pearson, R. G.; Mauermann, H. J. *J. Am. Chem. Soc.* **1982**, *104*, 500.
(6) (a) Yoshida, T.; Okano, T.; Otsuka, S. *J. Am. Chem. Soc.* **1980**, *102*, 5966. (b) Yoshida, T.; Okano, T.; Ueda, Y.; Otsuka, S. *J. Am. Chem. Soc.* **1981**, *103*, 3411.
(7) Kaspar, J.; Spogliarich, R.; Mestroni, G.; Graziani, M. *J. Organomet. Chem.* **1981**, *208*, C15.
(8) (a) Cheng, C. H.; Hendriksen, D. E.; Eisenberg, R. *J. Am. Chem. Soc.* **1977**, *99*, 2791. (b) Baker, E. C.; Hendriksen, D. E.; Eisenberg, R. *Ibid.* **1980**, *102*, 1020.
(9) Cheng, C. H.; Eisenberg, R. *J. Am. Chem. Soc.* **1978**, *100*, 5968.
(10) Cole-Hamilton, D. J. *J. Chem. Soc., Chem. Commun.* **1980**, 1213. Choudhury, D.; Cole-Hamilton, D. J. *J. Chem. Soc., Dalton Trans.* **1982**, 1885.
(11) Chan, S. F.; Chou, M.; Creutz, C.; Matsubara, T.; Sutin, N. *J. Am. Chem. Soc.* **1981**, *103*, 369 and references therein.
(12) Chou, M.; Creutz, C.; Mahajan, D.; Sutin, N.; Zipp, A. P. *Inorg. Chem.* **1982**, *21*, 3989.
(13) Marnot, P. A.; Ruppert, R. R.; Sauvage, J.-P. *Nouv. J. Chim.* **1981**, *5*, 543.
(14) McCleverty, J. A.; Wilkinson, G. *Inorg. Synth.* **1966**, *8*, 211.
(15) (a) Martin, B.; McWhinnie, W. R.; Waind, G. M. *J. Inorg. Nucl. Chem.* **1961**, *23*, 207. (b) Oliver, F. D.; Miller, J. D. *J. Chem. Soc., Dalton Trans.* **1972**, 2473.
(16) Balch, A. L.; Cooper, R. D. *J. Organomet. Chem.* **1979**, *169*, 97.
(17) Lawson, D. N.; Wilkinson, G. *J. Chem. Soc.* **1965**, 1900.
(18) Reddy, G. K. N.; Susheelamma, C. H. *J. Chem. Soc., Chem. Commun.* **1970**, 54.
(19) Kingston, J. V.; Scollary, G. R. *J. Chem. Soc., Chem. Commun.* **1970**, 670. Kingston, J. V.; Mahmound, F. T.; Scollary, G. R *J. Inorg. Nucl. Chem.* **1972**, *34*, 3197.

0020-1669/85/1324-2063$01.50/0

weighed into a solvent and water was added. After thorough stirring of the solution with both stopcocks closed, the flask was taken out of the glovebox and connected to the vacuum line. The solution was degassed and charged with the desired pressure of CO. The gas in the flask was sampled and analyzed by gas chromatography, and the flask was placed in an oil bath. The reaction temperature was maintained at ±2 °C by continuously stirring the oil bath as well as the reaction mixture. For all the data reported later each run was followed as a function of time: 300-mL flasks containing 25 mL of solution were used. For sampling, the flask was cooled to room temperature, a syringe was flushed and charged with 0.1–0.4 mL of argon, and then 0.1–0.4 mL of gas (CO_2 + H_2 + CO + (Ar)) was withdrawn from the vessel and analyzed. No adventititious N_2 was found. The rates were determined from the slopes of plots of micromoles of H_2(CO) vs. time.

Stoichiometry. The stoichiometry of the reaction of $Rh(bpy)_2^+$ with CO in different solvents at room temperature was established with use of a flat-bottomed flask (~40 mL) consisting of a side bulb and topped by a large-bore glass stopcock capped with a septum. In the argon-filled glovebox, the rhodium complex was weighed and transferred into the side bulb, 20 mL of solvent was added to the flask, and the flask was closed. After the flask was taken out of the glovebox, 2 mL of argon was replaced with 2 mL of CO by a syringe (~0.1 atm of CO). After the solvent was stirred for a few minutes, the gas in the flask was analyzed by gas chromatography using He as carrier gas and the CO to Ar ratio determined. The solid in the side bulb was then mixed with the solvent. The resulting solution was stirred for a few minutes, the gas was again analyzed, and uptake of CO by the solid was calculated by difference.

Gas Analysis. A Varian Series 1400 gas chromatograph fitted with a thermal conductivity detector and a molecular sieve 5A column (2 m × 3 mm) to analyze H_2 and CO and a Chromosorb 102 column (4 m × 3 mm) to analyze H_2, CO, and CO_2 was used. Argon was usually used as carrier gas. Gas samples (0.1–0.4 mL) were taken with Pressure-Lok air-tight gas syringes obtained from Precision Sampling Corp. A gas mixture (CO, CO_2, H_2, Ar) of known composition was used to calibrate all experiments. Liquid samples were analyzed on a Perkin-Elmer Sigma 3B gas chromatograph connected to a Sigma 10B data station and fitted with either an OV101 or an OV210 column.

The infrared spectra were recorded on a Nicolet MX-1 FT spectrometer as Nujol mulls between CsI plates. UV–vis measurements were done on Cary 17 and Cary 210 spectrometers. Microanalyses were performed by Schwarzkopf Microanalytical Laboratory and E. Norton of this department. Normally pH measurements were made on solutions cooled to room temperature.

Results and Discussion

General Features. Exposure of a purple solution of $[Rh(bpy)_2]Cl$ in ethanol–water to carbon monoxide immediately gave a green solution. When such a solution was stirred at 50–95 °C under CO for several days, H_2 and CO_2 were produced as expected for eq 1. The results of a preliminary survey of conditions for WGS activity of the system are presented in Supplementary Table I and are summarized first. The system operates efficiently under rather mild conditions (<100 °C (<1 atm CO)), and turnover numbers up to 3 h^{-1} are obtained at 95 °C. With 10% water by volume, the rate of product formation and the color of the solution remained essentially unchanged when ethanol was replaced by either 2-methoxyethanol ((2-OMe)EtOH) or 2-ethoxyethanol solvent. Similarly, H_2 and CO_2 were produced when the solvent was *p*-dioxane or ethylene glycol, but the rate decreased substantially in *N,N*-dimethylacetamide. With the alcohol–water mixtures, rates were greater with 10–50% alcohol than in pure water and greatest in weakly acidic solution (pH ~4), being negligible in both basic (pH >12)[20] and strongly acidic (pH <1) solutions.

Blank experiments were done as follows: (a) no rhodium catalyst added; (b) no CO gas added (the solution was under Ar); (c) no water added. On analysis of the gas phase, no H_2 (<10^{-3} mL) was detected in each case and no solvent degradation products (resulting from dehydrogenation of alcohols etc.) were observed when the final solutions were analyzed by GC.

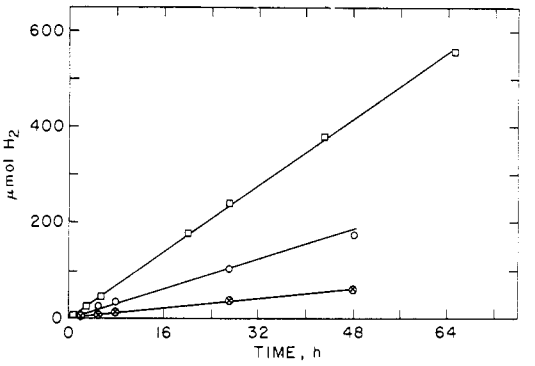

Figure 1. H_2 formation as a function of time at 0.8 atm CO with 2 × 10^{-4} M $[Rh(bpy)_2]Cl$, pH (at 90 °C): □, 3.4; ○, 2.7; ⊗, 2.1.

The yield of CO_2 was 1.0 ± 0.1 that for H_2 and was typically 0.95 in 15:10 ethanol–water. The pH of the reaction solution (at ~22 °C) after a 20-h run at 90 °C was 4.0–4.7 with 15:10 ethanol–water as solvent and 5.4 in 3:22 ethanol–water and did not change with reaction time. When H_2O was replaced by D_2O, the "hydrogen" produced was >70% D_2, indicating the source of H_2 to be water or water-exchangeable protons as from the –OH group of alcohols.

No change in rate was obtained when the solutions were filtered after 18-h reaction time, recharged with CO, and run for another 7 days. In cases where some solid was observed after long periods of time, the catalytic activity of the solid was tested in a separate experiment but no activity was found. The rates were comparable for the sulfate and chloride salts of $Rh(bpy)_2^+$ (both of which gave no precipitate), but use of the perchlorate salt led to precipitation of the reaction intermediates and much lower WGS rates.

Several other rhodium(I) systems were also assayed as catalysts for the WGS reaction (Supplementary Table II). The turnover rate decreased more than a factor of 10 when $Rh(bpy)_2^+$ was replaced with $Rh(phen)_2^+$ as catalyst precursor. The $[Rh(CO)_2Cl]_2$ complex was almost inactive, but some WGS activity was observed when bpy, phen, or Me_2bpy was added to alcohol–water solutions of the $[Rh(CO)_2Cl]_2$ dimer (Rh:L = 1:1), with the reactivity order L = bpy > Me_2bpy > phen. The $[Rh(CO)_2Cl]_2$(μ-4,4′-bpy)complex also showed catalytic activity but that of $[Rh(CO)_2Cl]_2$(μ-pz) was negligible.

Detailed Studies with $Rh(bpy)_2^+$ in Ethanol–Water Media. Since the alcohol–water mixtures showed high water gas shift activity over long times with $Rh(bpy)_2^+$ as catalyst precursor, these were subjected to detailed study. As mentioned above, the stoichiometry of eq 1 was found to hold within experimental error. At 90 °C in buffered 3:22 ethanol–water the H_2:CO_2 ratio after a 20-h run (2 × 10^{-4} M Rh(I), 0.8 atm CO) was as follows (pH, H_2:CO_2); 1.97, 1.07; 3.2, 1.08; 4.35, 0.95; 5.96, 1.21; 7.28, 1.2; 9.40, 1.0. The H_2:CO_2 ratio did not change with time (cf. Figure S1 which summarizes data obtained over 150 h for 15:10 ethanol–water media at 90 °C), and all of the systems were stable for long times and many turnovers as is illustrated in Figure 1 for buffered 3:22 ethanol–water at different pHs. Since 5 μmol of H_2 corresponds to one turnover (mol H_2/mol Rh) for the conditions used in Figure 1, it is also apparent that the system is genuinely catalytic; indeed the highest pH 3 point corresponds to >100 turnovers of the catalytic species.

To determine the rate law for the catalysis, a series of runs were carried out in 300-mL flasks containing 25 mL of solution. The added $[Rh(bpy)_2]Cl$ was varied between 0.2 × 10^{-3} and 1.2 × 10^{-3} M, the CO pressure (at 22 °C) was varied between 0.2 and 0.8 atm, and the amounts of H_2 and CO_2 produced after 20–22 h were measured. In all of the media investigated in detail, the H_2(CO_2) formation rates exhibit a linear dependence on the catalyst precursor concentration below ~1 × 10^{-3} M Rh[21] but

(20) (a) Note, however, that high-pH results are difficult to interpret because of parallel consumption of CO by direct reaction with hydroxide ion to give formate. From the literature rate constant and activation energy for the reaction of CO with OH^- (rate = $kP_{CO}[OH^-]$, k = 2.7 × 10^{-5} atm^{-1} s^{-1}, E_a = 22 kcal mol^{-1})[20b] the half-life for CO and OH^- consumption to give formate is initially ~2 h in run 19 (Tables SI) and after the 21-h run P_{CO} ~0.4 atm and $[OH^-]$ ~ 0.05 M with $[HCO_2^-]$ ~ 0.25 M. Thus, the strongest conclusion that can be drawn from the diminished H_2, in light of the above considerations, is that OH^- does not markedly enhance the H_2 evolution rate. (b) Iwata, M. *Chem. Abstr.* **1969**, *70*, F6989*v*.

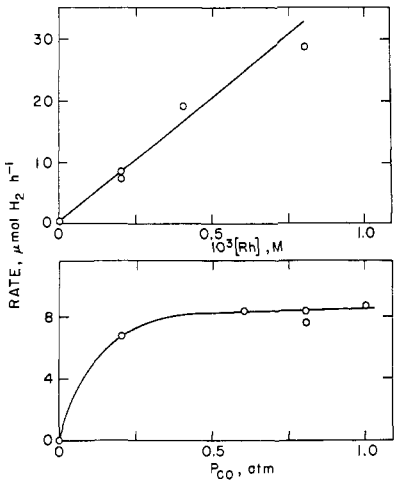

Figure 2. Characteristics of the pH 3.4, 3:22 ethanol–water system at 90 °C: top, H_2-formation rate vs. initial $[Rh(bpy)_2]Cl$ concentration with 0.8 atm CO; bottom, H_2-formation rate vs. CO pressure with 2×10^{-4} M $[Rh(bpy)_2]Cl$.

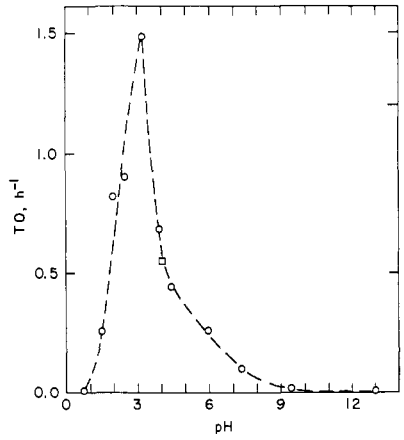

Figure 3. H_2-formation rate (mol of H_2/mol of Rh per hour) with 2×10^{-4} M $[Rh(bpy)_2]Cl$ initially, 0.8 atm CO, 90 °C , and 3:22 ethanol–aqueous buffer as solvent as a function of pH (measured at 90 °C). Each point was determined after a 20-h run. Other experiments at pH 1.5, 3.2, and 4.3 establish the rate to be independent of CO pressure under these conditions. The square point was determined with no added buffer.

are independent of CO partial pressure at moderately low CO. Data for buffered 3:22 ethanol–water at pH 3.0 are presented in Figure 2, and those for 15:10 and 3:22 ethanol–water mixtures containing no buffer, in Figures S2 and S3, respectively. [For

(21) As is shown in Figure S3, the H_2-formation rates in 3:22 ethanol–water (no buffer) appear to become independent of added $[Rh(bpy)_2]Cl$ above $\sim 10^{-3}$ M, suggesting that the catalyst activity decreases at high concentrations. The data are compatible with a monomer (M, active catalyst)–dimer (D, inactive in the WGS reaction) equilibrium:

$$M + H_2O + CO \xrightarrow{k_M} H_2 + CO_2 + M$$

$$M + M \rightleftharpoons D \quad (K_D)$$

A plot of TO^{-1} ((mol of H_2/h)/(mol of Rh taken) = TO) vs. [Rh] (insert in Figure S3) as suggested by the above scheme gives a good fit to the data. (The insert includes both H_2 and CO_2 points, with the latter giving a better fit to the model.) The reciprocal of the intercept gives $k_M = 1.08$ h^{-1} or 3.0×10^{-4} s^{-1}, and the slope-to-intercept ratio ($=2K_D$) gives $K_D = 760$ M^{-1}. The curve drawn through the points in the top of Figure S3 was calculated from these parameters. The value of k_M in 3:22 ethanol–water is thus very similar in magnitude to the first-order rate constant (3.5×10^{-4} s^{-1}) found above for 15:10 ethanol–water where the linear Rh dependence of the rate indicates oligomerization to be much less of a complication. This solvent-dependent dimerization is thus responsible for the lower WGS rates in water-rich media. Dimerization processes are also found in the $Rh(bpy)_2^+$ systems in the absence of CO[12] and are also suppressed by alcohol in the latter.

Table I. Carbon Monoxide Uptake by $[Rh(bpy)_2]Cl$ at Room Temperature[a]

medium[b]	mol of CO/ mol of Rh	medium[b]	mol of CO/ mol of Rh
pH 1.7	1.0	pH 10.8	1.7
pH 3.0	0.9	ethanol	1.5
pH 8.7	1.3		

[a] The [Rh(I)] was 2.5×10^{-4} M with 20 mL of solution, 23 mL of gas with initial partial pressure of CO of 0.1 atm and Ar of 0.9 atm. [b] The buffered solutions contain 2.4 mL of ethanol and 17.6 mL of aqueous buffers as follows: pH 1.7, 0.2 M sulfate; pH 3.0, 0.2 M phosphate, pH 8.7, 0.04 M borate; pH 10.8, 0.05 M carbonate.

the 15:10 ethanol–water medium, the temperature dependence of the rate in the CO-independent region was also investigated and k_{obsd} was found to be 3.8×10^{-5} s^{-1} (64 °C), 0.9×10^{-4} s^{-1} (71 °C), 1.6×10^{-4} s^{-1} (80 °C), and 3.5×10^{-4} s^{-1} (90 °C) (Figure S2), giving 21 ± 2 kcal mol^{-1} as the slope of a plot of ln (k/T) vs. $1/T$]. Finally, as indicated by the preliminary studies, the rates are pH dependent.

As is shown in Figure 3, the H_2/CO_2 production rate is negligible below pH 1 but rises with increasing pH, attaining a maximum near pH 3. At higher pH it drops off gradually and is negligible above pH ~9. The square at pH 4, determined without added buffer as in Figure S2, is seen to be very similar to the point with added buffer.

The data in Figures 2 and 3 show that the rate of the catalyzed WGS reaction is first order in catalyst precursor and independent of CO (above 0.3 atm). To clarify the nature of the catalytic pathway, knowledge of the complexes present under WGS conditions was sought.

Species in Solution under WGS Conditions. When solid $[Rh(bpy)_2]Cl$ is dissolved in CO-containing water, alcohol, or water–alcohol mixtures at room temperature, the UV–vis spectral changes indicate that rapid reaction takes place. Analysis of the depletion in the free CO level demonstrates, as shown in Table I, that 0.9–1.7 mol of CO react per mol of $[Rh(bpy)_2]Cl$ taken, depending upon the nature of the solution. The UV–vis spectra of solutions heated at 90 °C for >20 h (WGS runs) do not differ significantly from the initial room-temperature spectra,[22] indicating that the carbonyl complexes formed initially are those also present under WGS conditions. The product spectra and other observations depend, however, upon the pH of the medium.

pH <3. As shown in Table I, reaction of $Rh(bpy)_2^+$ with CO in acidic solution leads to the uptake of 1 mol of CO per mol of Rh(I) at room temperature. In addition, no bpy is released in this reaction (extraction of a pH 3 solution initially 2×10^{-4} M in $[Rh(bpy)_2]Cl$ with $CHCl_3$ before or after a WGS run yielded no bpy in the $CHCl_3$ extract despite the fact that >95% was extracted from 2×10^{-4} M bpy in the same buffer). The product species thus contains 2 mol of bpy and 1 mol of CO per mol of Rh(I) taken. The spectrum of the product solution has λ_{max} 244 nm, 304 ($\epsilon \sim 2 \times 10^{-4}$ M^{-1} cm^{-1} for both), and 380 ($\epsilon \sim 2 \times 10^3$ M^{-1} cm^{-1}) and is independent of pH below 3. Above pH 3, the 305- and 390-nm absorptions decrease in intensity.

pH >3. As shown in Table I, more than 1 (1.3–1.7) mol of CO is consumed per mol of Rh(I) taken. Furthermore, addition of CO induces release of bpy: when an unbuffered, pH 4–5, 3×10^{-4} M $[Rh(bpy)_2]Cl$ solution in 10 mL of water was stirred 30 min under 1 atm CO and then extracted with 30 mL of

(22) In a number of runs, absorption peaks indicative of $Rh(bpy)_2(H_2O)_2^{3+}$ or $Rh(bpy)_2(OH)_2^+$,[11] depending on the pH, were found. The peak magnitudes were consistent with oxidation of 10–20% of the added $[Rh(bpy)_2]Cl$ and were substantially reduced by scrubbing the CO used through $Cr(H_2O)_6^{2+}$ solutions. The oxidation is thus attributed to traces of O_2 in the CO. Neither $[Rh(bpy)_2(H_2O)_2](ClO_4)_3$ nor $[Rh(bpy)_3](ClO_4)_3$ is an active WGS catalyst in pH 3 3:22 ethanol–water mixtures: with 0.9 atm CO and 2×10^{-4} M Rh and at 90 °C, $Rh(bpy)_3^{3+}$ and $Rh(bpy)_2(H_2O)_2^{3+}$ produce <1% and <10% as much H_2, respectively, as $Rh(bpy)_2^+$ over 20 h. The activity reported for these complexes at higher pH[13] is undoubtedly due to more rapid reduction of Rh(III) to Rh(I) (rhodium(III) hydride) at the higher temperature and pH used in ref 13.

deaerated chloroform, the UV spectrum of the extract had λ_{max} of 232 and 282 nm, as expected for bpy, corresponding to ~0.6 mol bpy per mol of $Rh(bpy)_2^+$ initially present. In the spectrum of the aqueous layer from the extraction, peaks originally present at ~242 and 284 nm (bpy maxima in water) were absent, with peaks at 250, 300–310, and 385 nm remaining. Similar spectral behavior was found for a buffered 3:22 ethanol–water solution at pH 5.4. The higher pH species thus contain >1 mol of CO and <2 mol of bpy per mol of Rh(I).

The above observations demonstrate that the nature of the bpy- and CO-containing complexes is pH dependent. The fact that *low* pH favors metals binding of bpy is especially significant. The release of bpy from a metal complex should be favored at low pH because of protonation of the free ligand ($pK_a(bpyH^+) = 4.4$). The fact that bpy loss is suppressed by low pH in the present system strongly suggests formation of a rhodium(III) hydride (metal protonation) with a high affinity for bpy. Thus, the low-pH species is formulated as $Rh(bpy)_2(CO)H^{2+}$, a rhodium(III) carbonyl hydride. The fact that solution spectra change above pH 3 indicates that the pK_a of $Rh(bpy)_2(CO)H^{2+}$ (eq 2) is ~3;

$$Rh(bpy)_2(CO)H^{2+} \rightleftharpoons Rh(bpy)_2CO^+ + H^+ \qquad (2)$$

for comparison, the pK_a of $Rh(bpy)_2(H_2O)H^{2+}$ is 7.2.[12] The release of bpy then occurs from Rh(I) (eq 3, with S = solvent water

$$Rh(bpy)_2CO^+ + S \rightleftharpoons Rh(bpy)(CO)S^+ + bpy \qquad (3)$$

or alcohol). However, in view of the evidence for dimerization provided by the kinetic studies[21] and the fact that the uptake of >1 mol of CO per mol of Rh(I) is favored at higher pH (Table I), other processes (such as dimerization) may occur as well. Indeed, a green solid obtained on bubbling CO into a concentrated $[Rh(bpy)_2]Cl$ solution (0.1 g in 5 mL) in ethanol exhibits IR features (Nujol mull) characteristic of both bridging (1830 and 1805 cm^{-1}) and terminal (2060 and 1970 cm^{-1}) CO groups, consistent with the dimer formulation $[Rh(bpy)(CO)]_2CO^{2+}$. Because of the complexity of the higher pH solutions, we confine our modeling of the WGS catalysis in the next section to the low-pH region.

Mechanistic Considerations. Despite the complexity of the system, some tentative conclusions concerning the mechanism of the catalysis can be drawn from the lower pH data for 3:22 ethanol–water mixtures. Provided that the dominant form of the rhodium is $Rh(bpy)_2(CO)H^{2+}$, the rate data in Figure 2 and 3 give eq 4 as the limiting form of the rate law for $P_{CO} > 0.3$ atm,

$$d[CO_2]/dt = d[H_2]/dt = k[Rh(bpy)_2(CO)H^{2+}][H^+]^{-1} \qquad (4)$$

[Rh] $\leq 7 \times 10^{-4}$ M, pH <3, and 90 °C with $k \sim 10^{-6}$ M s^{-1} between pH 1.5 and 2.5. Equation 4 is consistent with the formation of a metallocarboxylic acid[23,24] as part of the catalytic sequence as shown in eq 5 or 5a. The $1/[H^+]$ dependence is

$$Rh(bpy)_2(CO)H^{2+} + OH^- \underset{k_{-1}}{\overset{k_1}{\rightleftharpoons}} Rh(bpy)_2(COOH)H^+ \qquad (5)$$

$$Rh(bpy)_2(CO)H^{2+} + H_2O \rightleftharpoons Rh(bpy)_2(COOH)H^+ + H^+ \qquad (5a)$$

$$Rh(bpy)_2(COOH)H^+ \overset{k_2}{\rightleftharpoons} Rh(bpy)_2H_2^+ + CO_2 \qquad (6)$$

consistent either with rate-determining formation of the metallocarboxylic acid (eq 5, $k = k_1/K_w$ where K_w is the water ionization constant at 90 °C) or with rate-determining decarboxylation of the metallocarboxylic acid (eq 6, $k = k_1k_2/k_{-1}$) present in pH-dependent equilibrium with $Rh(bpy)_2(CO)H^{2+}$ (eq 5a).[25,26] For a number of WGS-active metal carbonyls, hydroxide addition is rapid[4d,27,28] even at room temperature. Nevertheless, hydroxide addition can be rate determining under certain conditions,[4d] and our observations do not distinguish between eq 5 and 6 as rate-determining steps. Plausible steps completing the catalytic cycle are given in eq 7–9. Release of H_2, from the dihydride (eq 7)

$$Rh(bpy)_2H_2^+ \xrightarrow{k_3} Rh(bpy)_2^+ + H_2 \qquad (7)$$

$$Rh(bpy)_2^+ + CO \xrightarrow{k_4} Rh(bpy)_2CO^+ \qquad (8)$$

$$Rh(bpy)_2CO^+ + H^+ \xrightarrow{k_5} Rh(bpy)_2(CO)H^{2+} \qquad (9)$$

is fairly rapid ($k_3 > 10^{-2}$ s^{-1} in ethanol at 25 °C).[12,29] Addition of CO to $Rh(bpy)_2^+$ is extremely rapid ($k_4 > 10^6$ M^{-1} s^{-1})[29] at room temperature, and it is likely that $k_5 > 10^1$ M^{-1} s^{-1}.[30] All of these reactions should be even more rapid at 90 °C. Thus, eq 7–9, which may be responsible for H_2 production and regeneration of the catalyst $Rh(bpy)_2(CO)H^{2+}$, are faster than the highest turnover numbers ($\sim 10^{-3}$ s^{-1}) found in this WGS system and are therefore consistent with eq 5 or 6 as rate-determining steps.

In summary, the metallocarboxylate mechanism (eq 5–9) is proposed for "$Rh(bpy)_2^+$" catalysis of the water gas shift reaction. While our observations implicate relatively high WGS activity for $Rh(bpy)_2(CO)H^{2+}$, formally a Rh(III) complex, the higher pH data suggest that the Rh(I) complexes present above pH 3 have little, if any, activity. A relatively higher activity for the rhodium(III) hydride seems reasonable since a 3+ metal center[8,26a] should be more effective than a 1+ center in activating bound CO toward nucleophilic attack by OH^- or H_2O.

Conclusions

Bis(bipyridine)rhodium(I) reacts with CO in aqueous media to give $Rh(bpy)_2(CO)H^{2+}$ and/or rhodium(I) bipyridine–carbonyl complexes depending upon the conditions. At 90 °C (0.3–1 atm

(23) We neglect the possibility of a "formate mechanism":

$$CO + OH^- \rightarrow HCO_2^-$$

$$H^+ + HCO_2^- \xrightarrow{Rh} H_2 + CO_2$$

Such a pathway seems unlikely for the present system for several reasons: At low pH it is unlikely that HCO_2^- formation is sufficiently rapid to account for the observed rates.[20b] At room temperature $Rh(bpy)_2^+$ does not react with formate. At 90 °C (under Ar), Rh metal is gradually formed in the presence of formate (~0.8 M, pH ~8) and H_2 and CO_2 are produced. In the latter experiment it is not clear whether a rhodium complex or the metal is the catalyst for formate decomposition, but the latter seems likely since the rate of formate decomposition drops more than a factor of 10 when the solution is heated in the presence of CO. At pH ~3, under CO (0.8 M $NaHCO_2$ + 0.3 M H_2SO_4, 10:15 ethanol–water) the H_2 turnover is 0.45 h^{-1}, about as observed in the absence of formate (Figure 3) under comparable conditions. Thus, $Rh(bpy)_2(CO)H^{2+}$ does not appear to be a formate decomposition catalyst.

(24) Kang, H.; Mauldin, C.; Cole, T.; Slegeir, W.; Pettit, R. *J. Am. Chem. Soc.* **1977**, *99*, 8323.

(25) The following sequence provides an alternative decarboxylation mode:

$$Rh(bpy)_2(COOH)H^+ \rightleftharpoons Rh(bpy)_2(COO)H + H^+$$

$$Rh(bpy)_2(COO)H \rightleftharpoons Rh(bpy)_2H + CO_2$$

$$Rh(bpy)_2H + H^+ \rightleftharpoons Rh(bpy)_2H_2^+$$

Precedents for both eq 6 and the above mode have been established.[28]

(26) (a) Bercaw, J. E.; Goh, L.-Y. Halpern, J. *J. Am. Chem. Soc.* **1972**, *94*, 6534. (b) Grice, N.; Kao, S. C.; Pettit, R. *J. Am. Chem. Soc.* **1979**, *101*, 1627.

(27) Halpern, J. *Comments Inorg. Chem.* **1981**, *1*, 3.

(28) Gross, D. G.; Ford, P. C. *Inorg. Chem.* **1982**, *21*, 1702 and references therein.

(29) Zanella, A. W.; Mahajan, D., unpublished results.

(30) For $Rh(bpy)_2^+ + H_3O^+ \rightleftharpoons Rh(bpy)_2(H)H_2O^{2+}$ ($K = 2 \times 10^7$ M^{-1}),[12] the forward rate constant is $\sim 10^3$ M^{-1} s^{-1} at 25 °C: Zanella, A. W.; Creutz, C., manuscript in preparation. Thus, $k_5 > 10^1$ M^{-1} s^{-1} seems reasonable at 90 °C. Alternatively, the carbonyl hydride may be regenerated through the sequence

$$Rh(bpy)_2^+ + H_3O^+ \rightarrow Rh(bpy)_2(H)H_2O^{2+}$$

$$Rh(bpy)_2(H)H_2O^{2+} + CO \rightarrow Rh(bpy)_2(CO)H^{2+} + H_2O$$

The second reaction is complete in a few minutes or less at room temperature (1 atm CO) and so is certainly sufficiently rapid to sustain the catalytic chain at 90 °C.

CO), $Rh(bpy)_2(CO)H^{2+}$ is a relatively efficient catalyst for the water gas shift reaction (~1 turnover/h). The pH dependence of the catalytic rates (maximum at pH 3) suggests that either metallocarboxylic acid formation or decarboxylation is rate determining.

Acknowledgment. This work was performed at Brookhaven National Laboratory under Contract DE-AC02-76CH00016 with the U.S. Department of Energy and supported by its Division of Chemical Sciences, Office of Basic Energy Sciences.

Registry No. Rh, 7440-16-6; $[Rh(bpy)_2(CO)H]^{2+}$, 96293-15-1; $[Rh(bpy)_2]^+$, 47386-82-3; $[Rh(phen)_2]^+$, 56713-18-9; $[Rh(Me_2bpy)_2]^+$, 96293-16-2; $[Rh(CO)_2Cl]_2(\mu$-4,4'-bpy), 26173-13-7.

Supplementary Material Available: Table SII giving WGS reaction data and Figures S1–S3 giving hydrogen production rates as a function of solvent, temperature, rhodium concentration, and CO pressure (7 pages). Ordering information is given on any current masthead page.

Contribution from the Institute of Inorganic Chemistry, University of Basel, CH-4056 Basel, Switzerland

Ternary Complexes in Solution. 45.[1] Intramolecular Aromatic-Ring Stacking Interactions in Dependence on the Ligand Structure, Geometry of the Coordination Sphere of the Metal Ion, and Solvent Composition

RAMAN MALINI-BALAKRISHNAN, KURT H. SCHELLER, ULRICH K. HÄRING, ROGER TRIBOLET, and HELMUT SIGEL*

Received June 26, 1984

Stability constants of mixed-ligand M(phen)(PheCA)$^+$ complexes (M = Cu^{2+}, Zn^{2+}; phen = 1,10-phenanthroline; $PheCA^-$ = benzoate, 2-phenylacetate, 3-phenylpropionate, 4-phenylbutyrate, 5-phenylvalerate, 6-phenylcaproate) have been determined by potentiometric pH titration in aqueous solution and in 50% (v/v) ethanol- or dioxane/water and compared with the stabilities of the corresponding formate or acetate complexes. The ternary complexes containing phenylalkanecarboxylates ($PheCA^-$) are significantly more stable due to intramolecular stacking between the phenyl residue of the $PheCA^-$ ligands and the phen molecule. The formation degree of the intramolecular stacks in the Cu^{2+} and Zn^{2+} complexes was calculated, and the position of the intramolecular equilibrium between the opened and stacked isomer was determined: the stacked isomers occur between about 15 and 60% depending on the geometry of the coordination sphere of the bridging metal ion (Cu^{2+} (tetragonal)/Zn^{2+} (tetrahedral or octahedral)) and on the number of methylene groups between the phenyl residue and the coordinating carboxylate group (the "best fit" is usually reached with 2-phenylacetate). Addition of ethanol or dioxane to an aqueous solution may further favor intramolecular stack formation, contrary to the experience with simple unbridged binary stacking adducts, which are destabilized by the addition of ethanol or dioxane. The introduction of substituents into the phenyl residue of 2-phenylacetate influences the stability of the intramolecular stacks; especially a nitro group in the para position reduces considerably its formation degree. Replacement of the phenyl residue by the larger naphthyl moiety favors stacking and in 50% aqueous dioxane formation degrees of nearly 80% are reached, e.g., in Cu(phen)[2-(α-naphthyl)acetate]$^+$. The indole residue exhibits similar stacking properties. With regard to the side chains of amino acids it is interesting to note that the tendency to form intramolecular stacks in ternary complexes decreases in the series indole > phenyl > imidazole; the position of the last residue is based on measurements carried out with a pyrrole derivative as model ligand.

Metal ions are able to promote hydrophobic and aromatic-ring stacking interactions between suitable groups of different molecules, provided these molecules contain also ligating sites that allow the formation of mixed-ligand complexes.[2] Examples are the intramolecular ligand/ligand interactions within ternary complexes between suitable side chains of coordinated amino acids[3,4] or the corresponding interactions in mixed-ligand complexes of nucleotides and amino acids.[2,4] The systems mentioned are all of great interest with regard to biological systems.[5] However, due to the complicated nature of the ligands involved, it is difficult to study systematically the effect of structural alterations.

To overcome this handicap and to learn something about the factors that govern the formation degree of intramolecular aromatic-ring stacks, we initiated a comprehensive study that involves the components shown in Chart I. The series of phenylalkanecarboxylate ligands ($PheCA^-$)[6] allows a systematic variation of

Chart I

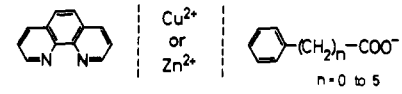

the distance between the coordinating carboxylate group and the phenyl moiety, which may form stacks with the also metal ion coordinated 1,10-phenanthroline. Indeed, in Cu(phen)(PheCA)$^+$ in aqueous solution intramolecular stacking interactions occur,[1] and the extent depends on the number of methylene groups be-

(1) Part 44: Dubler, E.; Häring, U. K.; Scheller, K. H.; Baltzer, P.; Sigel, H. *Inorg. Chem.* **1984**, *23*, 3785–3792.
(2) Sigel, H.; Fischer, B. E.; Farkas, E. *Inorg. Chem.* **1983**, *22*, 925–934.
(3) Fischer, B. E.; Sigel, H. *J. Am. Chem. Soc.* **1980**, *102*, 2998–3008.
(4) Sigel, H. In "Coordination Chemistry-20"; Banerjea, D., Ed.; Pergamon Press (IUPAC): Oxford, New York, 1980; pp 27–45.
(5) Hélène, C.; Lancelot, G. *Prog. Biophys. Mol. Biol.* **1982**, *39*, 1–68.

(6) Abbreviations: Ac^-, acetate; $ArCA^-$, arylalkanecarboxylate, e.g., α-$NPAc^-$, PAc^-; bpy, 2,2'-bipyridyl; Bz^-, benzoate; CA^-, carboxylate ligand; IAc^-, 3-indoleacetate; IPr^-, 3-indolepropionate; L, general ligand; M^{2+}, general divalent metal ion; MBz^-, *p*-methylbenzoate; $MOPAc^-$, 2-(*p*-methoxyphenyl)acetate; $MPSAc^-$, carboxylatomethyl *p*-methylphenyl sulfide; NBz^-, *p*-nitrobenzoate; $NPAc^-$, 2-(*p*-nitrophenyl)acetate; α-$NPAc^-$, 2-(α-naphthyl)acetate; β-$NPAc^-$, 2-(β-naphthyl)acetate; $NPSAc^-$, carboxylatomethyl *p*-nitrophenyl sulfide; PAc^-, 2-phenylacetate; PBu^-, 4-phenylbutyrate; PCa^-, 6-phenylcaproate; $PheCA^-$, phenylalkanecarboxylates, e.g. Bz^-, PAc^-, etc.; phen, 1,10-phenanthroline; PPr^-, 3-phenylpropionate; Pr^-, propionate; $PSAc^-$, carboxylatomethyl phenyl sulfide (= 2-(phenylthio)acetate = phenylmercaptoacetate); PVa^-, 5-phenylvalerate; $PyAc^-$, 1-pyrroleacetate; $TMOPAc^-$, 2-(3,4,5-trimethoxyphenyl)acetate. For the structures of the carboxylate ligands see Charts I–III.

0020-1669/85/1324-2067$01.50/0